J. Hydrol. Hydromech., 62, 2014, 4, 334–342
DOI: 10.2478/johh-2014-0035

Effects of patterned *Artemisia capillaris* on overland flow resistance under varied rainfall intensities in the Loess Plateau of China

Guanhua Zhang[1, 2], Guobin Liu[2*], Liang Yi[3], Pingcang Zhang[1]

[1] Department of Soil and Water Conservation, Changjiang River Scientific Research Institute, Wuhan, Hubei 430010, China.
[2] State Key Laboratory of Soil Erosion and Dryland Farming on the Loess Plateau, Institute of Soil and Water Conservation, Chinese Academy of Sciences and Ministry of Water Resources, Yangling, Shaanxi 712100, China.
[3] Hubei Academy of Environmental Sciences, Wuhan, Hubei 430072, China.
* Corresponding author. Tel.: +86 02987012411. Fax: +86 02987012210. E-mail: gbliu@ms.iswc.ac.cn

Abstract: In this paper simulated rainfall experiments in laboratory were conducted to quantify the effects of patchy distributed *Artemisia capillaris* on spatial and temporal variations of the Darcy-Weisbach friction coefficient (f). Different intensities of 60, 90, 120, and 150 mm h^{-1} were applied on a bare plot (CK) and four different patched patterns: a checkerboard pattern (CP), a banded pattern perpendicular to slope direction (BP), a single long strip parallel to slope direction (LP), and a pattern with small patches distributed like the letter 'X' (XP). Each plot underwent two sets of experiments, intact plant and root plots (the above-ground parts were removed). Results showed that mean f for *A. capillaris* patterned treatments was 1.25–13.0 times of that for CK. BP, CP, and XP performed more effectively than LP in increasing hydraulic roughness. The removal of grass shoots significantly reduced f. A negative relationship was found between mean f for the bare plot and rainfall intensity, whereas for grass patterned plots f_r (mean f in patterned plots divided by that for CK) increased exponentially with rainfall intensity. The f –Re relation was best fitted by a power function. Soil erosion rate can be well described using f by a power-law relationship.

Keywords: Overland flow; Darcy-Weisbach friction coefficient; Patch pattern; Vegetation structure; Simulated rainfall; Loess Plateau.

INTRODUCTION

Soil erosion has become a serious eco-environmental problem of worldwide concern. It causes on-site loss of topsoil and poses threats to land productivity (Lieskovský and Kenderessy, 2014; Ziadat and Taimeh, 2013). This is especially true on the Loess Plateau of China, where erosion-prone area reached up to 472,000 km^2 and the area with soil erosion modulus higher than 8,000 tonnes km^{-2} yr^{-1} was approximate 91,200 km^2 in recent years (Wang and Shao, 2013; Zhao et al., 2013b). The intense soil erosion and frequent anthropogenic activities have caused the extreme degradation of both zonal vegetation and soil quality in this region. Therefore, large-scale revegetation has been carried out for the sake of preventing soil erosion and restoring degraded ecosystems (Chen et al., 2008).

Resistance to flow determines routing velocities and is of great importance both within stream channels and over hillslopes when making predictions of streamflow and soil erosion (Smith et al., 2007). Overland flow resistance can be divided into grain resistance, form resistance, wave resistance, and rain resistance (Abrahams et al., 1990). These resistances are affected by rainfall, flow regime, roughness elements at the soil surface (e.g. crop residues, rock fragments, vegetation, litter, microbiotic crusts, geotextiles), inundation of roughness element, rill development, sediment deposition, and so on (Knapen et al., 2009; Lane, 2005; Lawrence, 1997, 2000; Parsons et al., 1994; Zhang et al., 2010). Darcy-Weisbach friction coefficient (f), Chézy (C) and Manning′n are commonly used to model flow resistance (Smith et al., 2007; Zhang et al., 2010), and f is the most widely used due to its dimensionless expression and good physical meaning (Luo et al., 2009). Exploring overland flow resistance is critical for better understanding the hydrodynamic mechanisms of soil erosion processes and flow concentration over hillslopes (Jiang et al., 2012), hence contributes to recommend appropriate measures to protect soils and reduce their erodibility.

Previous research indicated that overland flow resistance mainly associated with flow Reynolds number (Re), and most reached a power-law fitting for f-Re relationship expressing as (Smith et al., 2007):

$$f = a\,Re^{x} \qquad (1)$$

where, a and x are regression parameters that is influenced by surface features and flow regime.

Emmett (1978) stated that this relation applied only for plane beds where the resistance to flow was entirely grain resistance, with $f \propto Re^{-1.0}$ for laminar flow and $f \propto Re^{-2.0}$ for turbulent flow. Roels (1984) found the exponent ranged from –0.07 to –0.90 without taking into account flow regime factor. Abrahams et al. (1992) reported that the f–Re relation for standard plane-bed was not ubiquitous, and either positive or negative relationships may fit in different conditions. Zhang (1999) found a critical slope, below which f–Re relationships are negative and over which these are positive.

Rainfall especially rainfall intensity has been regarded as a key factor related to runoff and erosion (Cerdà, 2002; Ziadat and Taimeh, 2013), and it inevitably influences overland flow resistance. Yoon and Wenzel (1971) and Shen and Li (1973) indicated that shallow flow resistance increased with rainfall intensity when Re < 2000, whereas rainfall influence could almost be ignored when Re > 2000. Emmett (1978) confirmed that as against non-rainfall experiments, flow resistance doubled in rainfall experiments. Chen and Yao (1996) supported this point, but they held that rainfall intensity was not the sole factor: the smoother the bed, the more additional resistance the rainfall would yield; and this effect became slight after slope gradient reached the designed value.

Vegetation (e.g. community structure, plant stems, leaves, litter, root, and distribution pattern) plays an important role in regulating hillslope hydrological processes (Cerdà, 1998; Kröpfl et al., 2013; Shoshany, 2012; Zhang et al., 2012a, b). The complex nature of vegetation effects on flow resistance has been investigated systematically. Concrete cubes (Herbich and Shulits, 1964), glass fiber (Abrahams et al., 1994), stone or gravel (Abrahams and Parsons, 1994; Cerdà, 2001), geotextile (Giménez-Morera et al., 2010; Knapen et al., 2009), grass cover (Li et al., 2007; Pan and Shangguan, 2006), and plastic pipes (Cao et al., 2010; Li, 2009) were used to simulate surface cover. However, most studies were conducted on gentle slopes, and it is very necessary to conduct research on steep slopes not only because they takes large area in hillslopes of China, but also for further calibrating the results of gentle slopes (Li et al., 2007).

Patched patterns of vegetation have been reported in many African and Australian arid and semi-arid areas since the 1950s (Beard, 1967; Dunkerley and Brown, 1995; Greenwood, 1957; Worrall, 1959). The typical characteristics of vegetation patterns in arid and semi-arid ecosystems are higher plant-cover patches that are mainly distributed in spots or bands as a mosaic (Aguiar and Sala, 1999; Kröpfl et al., 2013). Under some circumstances, plant species in these regions also had several different patterns of root distribution (Fowler, 1986; Nobel, 1990). Perennial root zones are wider and deeper than those of annuals, and phreatophytes are often very deep rooted (Vásquez-Méndez et al., 2011). Additionally, many studies also placed focus on the dynamics of the hydrological and erosional processes that generate and sustain patchiness (Boer and Puigdefábregas, 2005; Cerdà, 1997; Dunkerley and Brown, 1999; Puigdefábregas, 2005). The main idea drawn in these studies is that vegetation patches divide slopes into runoff and runon zones and consequently into erosion (bare) and deposition (vegetated) zones which act as source and sink, respectively (Cerdà, 1997; Dunkerley and Brown, 1995; Puigdefábregas, 2005). Dekker et al. (2007) reported that vegetation distribution is generally controlled by precipitation; meanwhile, precipitation distribution affects vegetation development and distribution, which in turn modifies the atmospheric energy and water storage. Bedford and Small (2008) found the spatial patterns of soil properties are assumed to be linked to patchy dryland vegetation. Hitherto, there is still a lack of information or direct experimental study in the Loess Plateau of China where the arid and semi-arid lands occupy about 67% of the entire region (Li et al., 2003).

As aforementioned, significant achievements have been made in exploring the flow resistance characteristics over last several decades, and numerous studies pertaining to vegetation impacts, especially grass cover, on flow resistance have also been conducted. Nevertheless, most research was on slopes with uniform distribution of different vegetation types, very few involving the effects of vegetation structures (surface vegetation and roots) in terms of hydrodynamics (De Baets et al., 2006; Fan and Chen, 2010). Plant canopy and root contribute differently in runoff and sediment reduction, and their respective influence mechanism also (Zhao et al., 2013a; Zhou and Shangguan, 2007). Particularly in Loess Plateau of China, plants are mostly well developed roots but thin canopy, for reducing transpiration to adapt to the dry climate (Zhao et al., 2013a). It is thus imperative to elucidate the hydrodynamic mechanism of vegetation structures on erosion control in this region.

Therefore, the objectives of this study were (i) to investigate the effects of patchy distributed *Artemisia capillaris* on spatial and temporal variations of the Darcy-Weisbach friction coefficient (f) under varied rainfall intensities; (ii) to analyze the effects of vegetation structures (*A. capillaris* and roots) being different patched patterns on f; (iii) to explore the relationships between f and rainfall intensity and flow regime under the experimental conditions. The findings can offer useful insights into the dynamic mechanism of soil erosion and provide scientific guidance for suitable land uses and construction of soil and water conservation measures.

MATERIALS AND METHODS

Simulated rainfall set-up

The study was carried out under simulated rainfall conditions and a side-sprinkle rainfall simulating set-up was used at the State Key Laboratory of Soil Erosion and Dryland Farming on the Loess Plateau, Yangling, China. Rainfall height was 16 m. The measured uniformity of simulated rainfall reaches > 85% of that of natural rainfall, which indicates the rainfall uniformity meets the experimental requirement. There was an operating system for rainfall controlling. Calibration of rainfall intensities was performed before each rainfall test. Experimental rainfall intensities can be obtained through adjusting nozzle combination and water pressure, which can generate different erosion forces and flow rate. And on this basis, we studied rainfall's impact on flow resistance.

Plot characteristics and experimental treatments

The experimental plots were made of steel sheets, with dimensions of 2 m×1 m. The slope gradient can be adjusted in the range of 0–25°, and 15° was selected in this study since it is a general gradient for returning farmland to forestland or grassland on the Loess Plateau of China. The soil tested was a silt loam (International Taxonomy) collected from 0–20 cm soil in an experimental field at An'sai, Shaanxi Province, China, and its sand, silt and clay contents were 46%, 46% and 8%, respectively. The soil was air-dried, gently crushed, and passed through a 10 mm sieve to remove gravel and residues. Before packing, a 10 cm layer of fine sand was put at the bottom of each plot for better drainage. Then 30 cm thick soil was packed in three 10-cm layers at a representative bulk density of 1.2 g cm^{-3}. Besides, each soil layer was raked lightly before the next layer was packed in case of discontinuity between them. *Artemisia capillaris*, a common indigenous grass on the Loess Plateau, was used for vegetation patterns. The grass seed was sown with a row spacing of 10 cm parallel to the plot surface and similar sowing density was adopted to ensure uniform grass coverage for all plots. After sowing, the plots were covered with straw mats and watered to promote germination and seedling growth.

It is estimated that the threshold coverage for vegetation influencing soil erosion varied from 30–50% (Guo, 2000). Based on the same coverage (50%) but different distribution patterns, five treatments were implemented in the study: bare soil as control (CK), a checkerboard pattern (CP), a banded pattern perpendicular to the slope direction (BP), a single long strip parallel to slope direction (LP), and a pattern with small patches distributed like the letter 'X' (XP) (Fig. 1). Vegetation cover was measured using vertical and aerial photographs taken with a high-resolution digital camera, as well as empirical estimation by visual observation. Four high rainfall intensities (60, 90, 120, and 150 mm h^{-1}) were selected in this study, since high-intense and short-duration rainstorms, which are primarily responsible

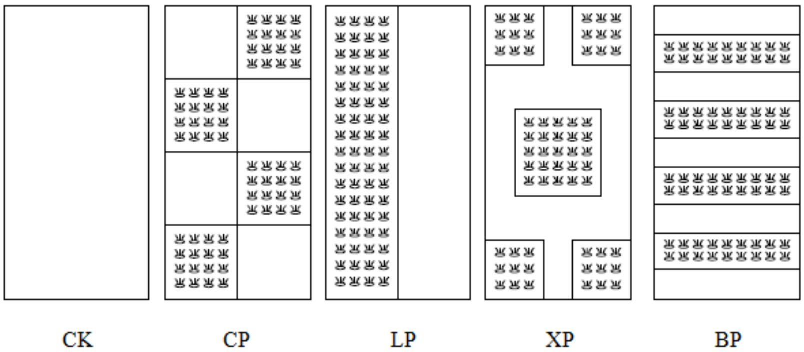

Fig. 1. Experimental treatments for different patched patterns of *Artemisia capillaris*.

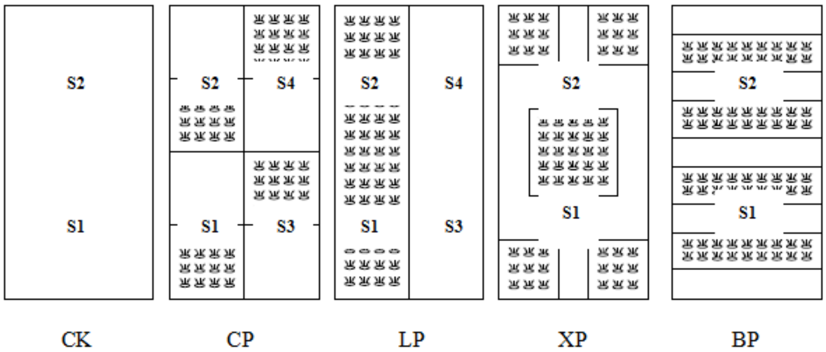

Fig. 2. Sketch map of section division for different treatments.

for soil erosion, frequently occur on the Loess Plateau. The experiment lasted 60 min after runoff initiation. All treatments were replicated three times.

Measurements and parameter calculation

For each rainfall simulation, plastic buckets were used to collect all runoff and sediment at the plot outlet at 3-min intervals. After the rainfall, runoff in each bucket was weighed on a balance. The buckets were then allowed to stand until the suspended sediment settled out. Then the supernatant was discarded, and the remaining wet sediment was transferred to iron basins to determine sediment weight after oven-drying at 105°C to constant weight. The dry sediment weight was then used to calculate sediment concentration and soil erosion rate.

Surface flow velocities (V_s) were measured by the $KMnO_4$ tracing method. The time of the tracer travelling across a marked distance (1 m) was determined according to the leading edge propagation using a stopwatch at 3-min intervals. From upslope to downslope, different longitudinal cross-sections were designed to determine velocities for different treatments (Fig. 2). Hence, for each rainfall event, 20 measurements were performed at each section, which were then averaged to obtain the mean surface flow velocity of this section.

Water temperature was measured during the experiments, which was used to calculate flow kinematical viscosity. Flow depth and Reynolds number (*Re*) were calculated from Eqs. (2) and (3), respectively:

$$h = \frac{Q}{V B t} = \frac{q}{V} \tag{2}$$

$$Re = V h / \upsilon = q / \upsilon \tag{3}$$

where, h is flow depth (m), Q is runoff volume during t time (l), V is mean flow velocity (m s^{-1}), q is unit discharge (m^2 s^{-1}), B is width of water-crossing section (m), and υ is kinematical viscosity (m^2 s^{-1}).

Measured V_s was used to estimate mean flow velocities (V) by multiplying a correction factor α according to flow regime (*Re*), with α being 0.67 for laminar, 0.7 for transitional flow, and 0.8 for turbulent flow, respectively (Luk and Merz, 1992). Under the experimental conditions, flow *Re* was 25–80 (Zhang, 2012), thus mean flow velocities were corrected using 0.67 and then used to determine other hydraulic parameters.

The Darcy-Weisbach friction coefficient (f) was calculated from Eq. (4):

$$f = \frac{8 g h J}{V^2} \tag{4}$$

where, J is flow energy gradient and is generally calculated as the sine value of slope gradient, g is gravitational acceleration (m s^{-2}).

To simulate vegetation structure, after the experiments with intact plants were completed, *A. capillaris* was clipped at the soil surface and only roots remained. All theses plots were subjected to the corresponding run tests again to investigate the flow resistance characteristics when surface condition changed. We referred to the plot with the intact plant and that with only the root as ‘plant plot’ and ‘root plot’, respectively.

Data analysis

Analysis of Variance (ANOVA) was used to detect treatment effects on measured variables. If significant treatment effects were observed ($p < 0.05$), the least significant difference (LSD) was used to test comparisons among treatment means. Paired sample *t*-tests were performed to analyze differences in variable means before and after clipping the above-ground parts of *A. capillaris*. These statistical analyses were performed using the SPSS 13.0 program.

RESULTS

Spatial variations of Darcy-Weisbach friction coefficient (*f*)

Grass patches generally had high effectiveness in increasing flow resistance (Table 1). The patterned plots of both plant and root plots had higher Darcy-Weisbach friction coefficients (*f*) than bare plots, and grass vegetated sections higher than bare ones. The *f* for different slope positions decreased substantially after removing above-ground portions of *A. capillaris*. For all treatments in plant plots, differences in *f* of lower slopes (S1/S3) were less than those of upper slopes (S2/S4). Mean *f* of the whole slope for patterned treatments was in the range of 2.8–9.1, which was 1.25–13.0 times of that for CK (Fig. 3). In addition, mean *f* of the whole slope was slightly different among treatments BP, CP, and XP, yet they were markedly higher than treatment LP. No statistical differences were detected between LP and CK. These results indicated that treatments BP, CP, and XP performed more effectively than LP in increasing hydraulic roughness, and thus more efficiently in flow retardation, which agrees with the findings of Zhang et al. (2012b).

Paired sample *t*-tests demonstrated that mean *f* significantly ($p < 0.05$) decreased after removing *A. capillaris* shoots clinging to the ground, and no differences in mean *f* were detected among patterned treatments. For the patterned treatments in root plots, mean *f* of the whole slope was 1.69–3.23, which was just 0.75–3.78 times of that for CK (Fig. 3). Besides, there were minor differences in *f* among longitudinal sections, which was not the case for intact plant plots. This indicated that grass roots made small contribution to hydraulic roughness, thus removal of grass shoots or/and leaves significantly affect overland flow resistance. This result also suggests that grass cutting or grazing is crucial for the performance of grass patches in retarding overland flow from severely eroded steep slopes.

Table 1. Darcy-Weisbach friction coefficient (*f*) for different slope positions.

RI	Vegetation pattern	Plant plots					Root plots				
		S1	S2	S3	S4	Mean	S1	S2	S3	S4	Mean
	CK	1.80	2.86			2.25Ca	1.80	2.86			2.25ABa
	CP	6.08	14.80	5.51	8.06	7.76Aa	1.76	3.22	1.72	2.81	2.26ABb
60	BP	5.03	5.79			5.39Ba	2.74	3.35			3.03Ab
	LP	7.68	10.22	1.18	1.29	2.81Ca	2.58	2.99	1.03	1.19	1.69Bb
	XP	4.38	13.08			7.20Aa	1.84	2.84			2.27ABb
	CK	0.95	2.91			1.58Ba	1.00	3.06			1.67Ba
	CP	7.46	16.47	3.02	11.94	7.60Aa	1.71	4.12	1.56	2.93	2.32ABb
90	BP	6.27	12.38			8.64Aa	3.03	3.45			3.23Ab
	LP	7.93	8.57	1.26	1.55	2.98Ba	2.48	3.27	1.20	1.64	1.95Bb
	XP	5.26	15.66			8.64Aa	1.88	3.55			2.54ABb
	CK	0.57	2.79			1.14Ba	0.61	2.96			1.21Ba
	CP	4.91	19.24	3.09	12.38	7.10Aa	3.02	3.80	2.01	2.76	2.80Ab
120	BP	4.95	9.84			6.85Aa	2.13	4.75			3.09Ab
	LP	3.00	4.88	1.20	4.22	2.79Ba	3.40	3.78	1.18	3.54	2.60ABa
	XP	3.62	11.09			6.02Aa	1.96	3.37			2.54ABb
	CK	0.40	1.35			0.70Da	0.40	1.35			0.70Ba
	CP	4.90	17.65	2.88	13.83	6.99Ba	2.19	3.06	1.37	2.85	2.22Ab
150	BP	6.01	13.93			8.89Aa	1.92	3.73			2.63Ab
	LP	3.06	8.62	1.46	2.95	3.06Ca	2.73	4.86	0.82	2.68	2.16Aa
	XP	4.66	21.80			9.13Aa	1.53	2.52			1.94Ab

Note: RI refers to rainfall intensity (mm h^{-1}). CK is bare plot as control; CP is a checkerboard pattern; BP is a banded pattern perpendicular to the slope direction; LP is a single long strip parallel to slope direction; and XP is a pattern with small patches distributed like the letter 'X'. S1, S2, S3, and S4 refer to four cross-sections distributed on different slope positions.
Within a column at the same rainfall intensity means followed by the same uppercase are not significantly different at $p< 0.05$ level using the least significant difference (LSD) method; within a row means followed by the same lowercase are not significantly different at $p< 0.05$ level using paired *t*-test method.

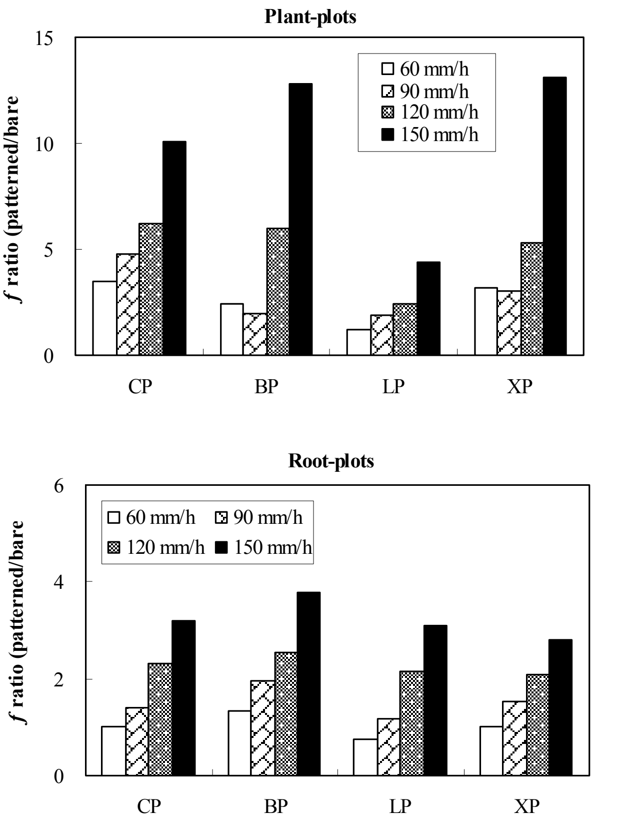

Fig. 3. Darcy-Weisbach friction coefficient (f) ratio of intact plant and root plots to bare soil.
CK is bare plot as control; CP is a checkerboard pattern; BP is a banded pattern perpendicular to the slope direction; LP is a single long strip parallel to slope direction; and XP is a pattern with small patches distributed like the letter 'X'.

Darcy-Weisbach friction coefficient (f) and rainfall intensity (RI)

Since mean f for the bare soil plot will respond differently to various rainfall conditions (e.g. rainfall intensity), the relative Darcy-Weisbach friction coefficient (f_r) was used instead of mean f to compare the resistance characteristics for different patched patterns and rainfall intensities. f_r was defined as the ratio between mean f for the patterned plots and the f for the bare soil plot, tested at the same rainfall intensity.

Mean f for bare soil and f_r for patterned soil surface were plotted against rainfall intensity (RI), respectively (Fig. 4). Exponential relationships, computed by non-linear regression analysis, are given below.

Bare plot $f = 4.994e^{-0.013RI}$ $(R^2 = 0.975, p < 0.01)$ (5)

Plant plots $f_r = 2.638+0.050e^{0.033RI}$ $(R^2 = 0.622, p < 0.01)$ (6)

Root plots $f_r = 0.387+0.746e^{0.011RI}$ $(R^2 = 0.907, p < 0.01)$ (7)

The results showed an exponential decline in mean f for bare soil, but an exponential increase in f_r for patterned plots, with increasing rainfall intensity. Small differences in f_r among patterned treatments could be observed under lower rainfall intensity, whereas this phenomenon increased under higher rainfall intensity (Fig. 4a). Removing the above-ground portions of *A. capillaris* not only reduced mean f in root plots, thus narrowing their inter-differences from the bare plot, but also lightened their within-differences among root plots (Fig. 4b).

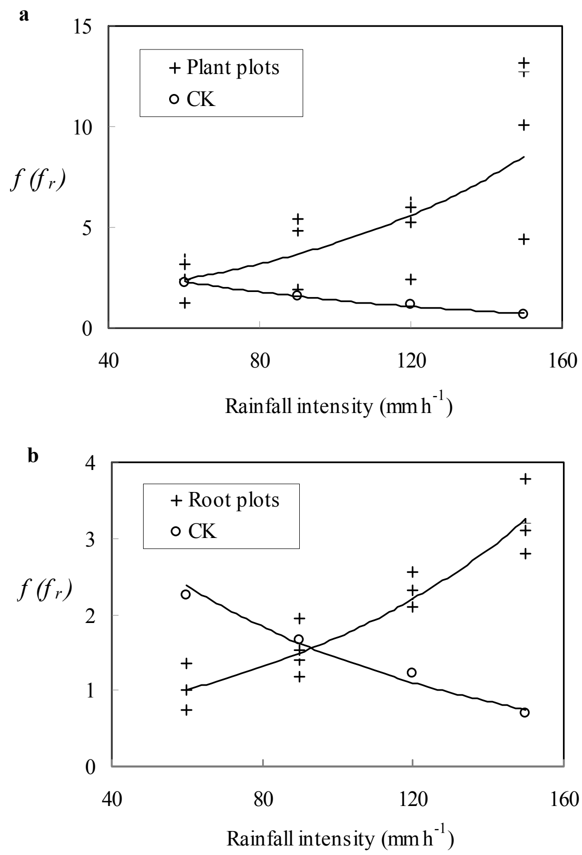

Fig. 4. Exponential relations between mean f for bare soil, f_r for both (a) intact plant plots and (b) root plots and rainfall intensity.

Darcy-Weisbach friction coefficient (f) and Reynolds number (Re)

In the current study, f–Re could be well described by power functions (Fig. 5).

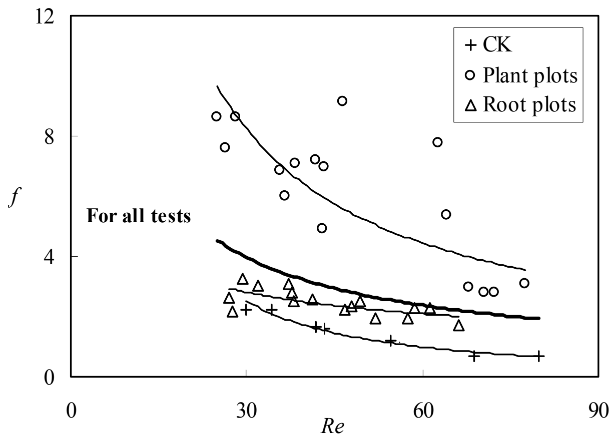

Fig. 5. Darcy-Weisbach friction coefficient (f) as a function of Reynolds number (Re).

The best fitting between f and Re for bare soil plot was:

$$f = 246.72Re^{-1.349} \quad R^2 = 0.961 \quad (8)$$

For intact plant patterned plots, it was:

$$f = 166.44Re^{-0.885} \quad R^2 = 0.593 \quad (9)$$

For the root patterned plots, it was:

$$f = 11.861Re^{-0.424} \quad R^2 = 0.472 \quad (10)$$

As can be seen in eqs. (8–10), the power parameters for intact plant and root plots were 0.885 and 0.424, respectively, and they were much smaller than that for bare soil plot (1.349). This indicates that *Re* was more sensitive to *f* for bare soil plots than plant and root plots, and *f* decreased with *Re* much faster for bare soil than the grass patterned soil surfaces. This is due to the decreased cover of bare soil strengthening raindrop splash and turbulence of overland flow, and further decreasing flow resistance. The fitted line of root plots was almost parallel to the *x*-axis of *Re* and varied within a small range, implying that *f* was nearly independent of flow regimes or *Re* when removing above-ground shoots and consequently further suggesting the vital function of above-ground portions of *A. capillaris* in overland flow resistance on hillslopes, as is in accordance with the aforementioned analysis.

For all tests, *f* decreased with *Re* following a power trend with the regression equation being $f = 53.677\ Re^{-0.757}$ ($R^2 = 0.141$), indicating that for patchy distribution of vegetation on hillslopes, *Re* may not be applied as an independent parameter to estimate *f* effectively and other factors should be taken into account in follow-up research.

Temporal variation

Due to the similar changing processes of flow resistance for each treatment under different rainfall intensities, this paper took 90 mm h^{-1} as an example to analyze temporal variations of flow resistance. Fig. 6 shows that Darcy-Weisbach friction coefficient (*f*) curves for root plots entirely declined compared with those for intact plant plots, thus indicating lower flow resistance when clipping shoots. The *f* processes were a little different among treatments, especially during the initial runoff period. The *f* in the XP plot decreased substantially at first, then fluctuated in the first 25 min of runoff, and thereafter became fairly steady. For other treatments, *f* firstly increased and then gradually tended to stabilize. This pattern disagrees with Li et al. (2007), who found runoff resistance on slope-gully surfaces with grass cover continuously increased with time. The differences in flow resistance processes may be attributed to differences in experimental conditions.

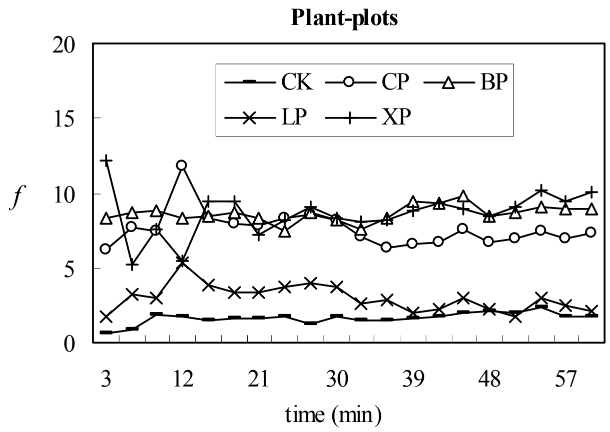

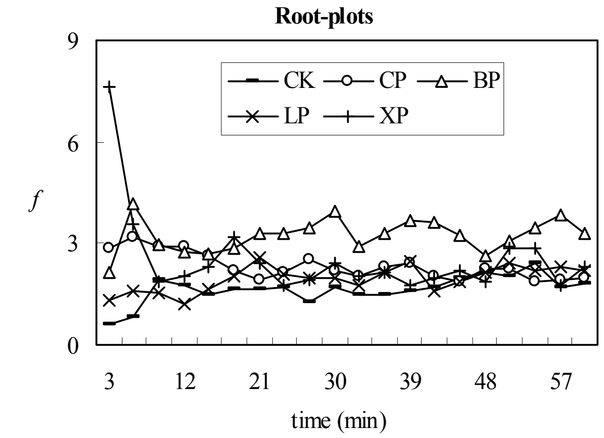

Fig. 6. Temporal variation in Darcy-Weisbach friction coefficient (*f*) for different treatments (A case study of 90 mm h^{-1}).
CK is bare plot as control; CP is a checkerboard pattern; BP is a banded pattern perpendicular to the slope direction; LP is a single long strip parallel to slope direction; and XP is a pattern with small patches distributed like the letter 'X'.

Overland flow is the result of an interaction between erosion dynamics and the underlying surface, and is inevitably subjected to a friction force to balance the gravity which acts to propel water downslope. Flow resistance characteristics therefore reflect erosion processes. The relationship between erosion rate (E_r) and Darcy-Weisbach friction coefficient (*f*) was further analyzed. As shown in Fig. 7, *f* was negatively correlated with erosion rate following a power function, with regression analysis of $E_r = 7.747f^{-1.083}$ ($R^2 = 0.764$, $n = 40$, $p < 0.01$).

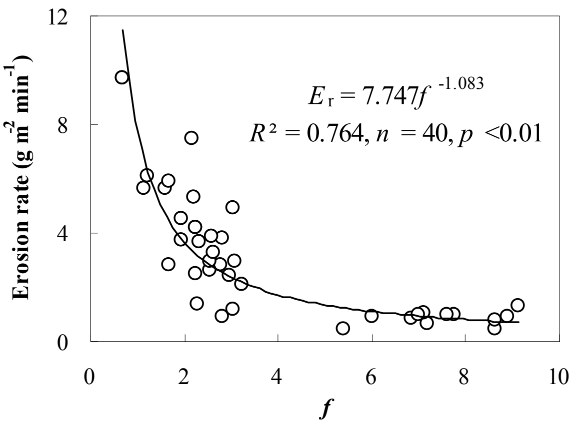

Fig. 7. Relationships between soil ersoion rate and Darcy-Weisbach friction coefficient (*f*).

DISCUSSIONS AND CONCLUSIONS

Darcy-Weisbach friction coefficients (*f*) reflect the underlying surface resistance to overland flow. Under the same hydrodynamic conditions, greater *f* implies more energy will be consumed to overcome flow resistance thus less energy is available for soil detachment and sediment transport, and consequently causes slight soil erosion. Our research confirms the importance of spatial discontinuities induced by patterned vegetation in hillslope runoff processes, showing that patched *A. capillaris* plots had higher *f* than bare soil plots, and grass vegetated sections higher than bare ones. Soil erosion rate can be well reflected using *f* by a negative power relation. Amongst the grass patterns, BP, CP, and XP performed more effectively than LP in increasing flow resistance. Grass cutting significantly reduced *f* and minor differences in *f* were observed between root plots and bare soil plots, implying that a greater shoots/ground cover and roots in vegetation patches, behaving as intercepting rainfall, dissipating raindrop energy, promoting flow resistance, reducing overland flow velocities and hydraulic shear stresses, and soil fixation and slope stabilization, diminished soil erosion potential (Erpul et al., 2002; Regüés and Torri, 2002; Vásquez-Méndez et al., 2010; Zhang et al., 2012a, b). These are indicative of the importance of vegetation cover in regulating runoff processes as also observed by Wainwright et al. (2002) and Bautista et al. (2007), and reflects the importance of the patchy vegetation in the hydrological functioning of an environment (Beskow et al., 2009; Irvem et al., 2007). Actually, in areas with a patchy distribution of vegetation, the relationships between runoff-erosion rates and vegetation covers are even more pronounced, and there are different hydrological and erosional responses to different patterning surfaces (Cerdà, 1997).

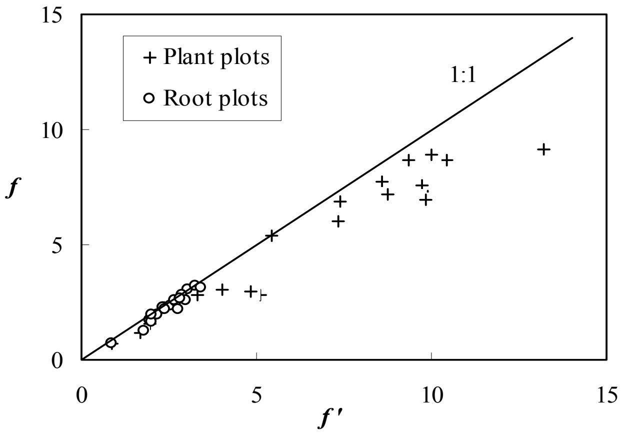

Fig. 8. Comparison of overland flow resistance based on different computing methods.

Numerous studies have explored the effect of rainfall on overland flow resistance. However, on rough erodible beds, quantifying this effect is beset with many complications, so no final conclusion has yet been reached. This study found that mean *f* of the whole slope for bare soil plot was negatively correlated with rainfall intensity following an exponential function, whereas positively exponential functions fitted well between relative f (f_r) and rainfall intensity for patterned plots. The result is inconsistent with many previous studies that took other factors into account, such as flow regime (Savat, 1977; Shen and Li, 1973), surface roughness (Chen and Yao, 1996), raindrop splash intensity (Mei, 2004), and slope gradient (Pan and Shangguan, 2009). Besides, the current study used a common method that calculated *f* from mean input parameters of the whole slope. As against this method, a second method was proposed whereby mean *f* was determined by averaging the respective *f* throughout flow cross-sections, which hereinafter is referred to as f'. Under the experimental conditions, almost all *f* values were less than f' with the points being scattered for intact plant plots, whereas *f* approximated f' with the points being more concentrated and closer to the 1:1 line for root plots (Fig. 8). Yi et al. (2011) reported that on a smooth flume of 15°, *f* was less than f', but the two values were basically identical on 20°, and when 25° was set, *f* was generally greater than f', indicating the importance of slope gradient in determining the Darcy-Weisbach friction coefficient (*f*). This again suggests a complex effect of rainfall that involves many aspects.

As for *f*–*Re* relation, overland flow is far complex than streamflow. At present a relatively consistent view point is that dividing overland flow resistance according to surface features using open channel hydraulics, and then performing superposition to obtain the resistance (Jiang et al., 2012). Our results agree with previous studies in the relation form as eq. (1) but different in the power parameters. Abrahams et al. (1992) studied the flow resistance of non-vegetated soil in Arizona and found the power parameter *x* in eq. (1) varied from –0.43 to –1.10 with the mean value being –0.81, which is much greater than eq. (8) of our study. Their further research (Abrahams et al., 1994) demonstrated that *f*–*Re* relation was positive for grassland but negative for shrubland. Roels (1984) considered slope length as an important factor of *f*–*Re* relation thus the *f*–*Re* relation for long slope couldn't obtain by interpolating and extrapolating. These differences may be attributed to rainfall, underlying surface, vegetation type, slope feature, etc. and/or their interaction, showing *Re* may not be used as an independent parameter to effectively estimate *f* and some other factors may need to be considered in further research.

In conclusion, many factors as rainfall, Reynolds number, vegetation, slope, and their interaction affect Darcy-Weisbach friction coefficient. Most achievements based on specific experimental condition and it is difficult to reveal its inherent law. Further research, such as a more strategic variety of treatments (e.g. multiple slope gradients, one vegetation pattern with different-sized gaps or planting density, soil-bins or flumes, simulated rainfall or scouring, smooth bed or rough bed), should be conducted to elucidate the mechanisms.

Acknowledgement. This research was supported by the National Natural Science Foundation of China (No. 41301298; 41271303; 41301296; 41201268), the Basic Research Fund for Central Public Research Institutes (No. CKSF2014025/TB) and the Special Fund of Strategic Priority Research Program of the Chinese Academy of Sciences (No. XDA05060300).

REFERENCES

Abrahams, A.D., Parsons, A.J., 1994. Hydraulics of interrill overland flow on stone-covered desert surfaces. Catena, 23, 111–140.

Abrahams, A.D., Parson, A.J, Luk, S.H., 1990. Field experiments on the resistance to overland flow on desert hillslopes. IAHS Publication, 189, 1–18.

Abrahams, A.D., Parsons, A.J., Hirsch, P.J., 1992. Field and laboratory studies of resistance to interrill overland flow on semiarid hillslopes, Southern Arizona[C]//Overland Flow: Hydraulics and Erosion Mechanics. UCL, London, pp. 1–24.

Abrahams, A.D., Parson, A.J., Wainwright, J., 1994. Resistance to overland flow on semiarid grassland and shrubland hillslopes. J. Hydrol., 156, 431–446.

Aguiar, M.R., Sala, O.E., 1999. Patch structure, dynamics and implications for the functioning of arid ecosystems. Tree, 14, 273–277.

Bautista, S., Mayor, A.G., Bourakhouadar, J., Bellot, J., 2007. Plant spatial pattern predicts hillslope runoff and erosion in a semiarid Mediterranean landscape. Ecosystems, 10, 987–998.

Beard, J.S., 1967. A study of patterns in some Western Australian heath and mallee communities. Australian Journal of Botany, 15,131–139.

Bedford, D.R., Small, E.E., 2008. Spatial patterns of ecohydrologic properties on a hillslope-alluvial fan transect, central New Mexico. Catena, 73, 34–48.

Beskow, S., Mello, C.R., Norton, L.D., Curid, N., Violab, M.R., Avanzia, J.C., 2009. Soil prediction in the Grande River Basin, Brazil using distributed modelling. Catena, 79, 49–59.

Boer, M., Puigdefábregas, J., 2005. Effects of spatially structured vegetation patterns on hill-slope erosion in a semiarid Mediterranean environment: a simulation study. Earth Surf. Process. Landforms, 30, 149–167.

Cao, Y., Zhang, G.H., Tang, K.M., Luo, R.T., 2010. Impact of simulated surface cover on resistance coefficient of overland flow. Journal of Soil and Water Conservation, 24, 86–89. (In Chinese with English Abstract.)

Cerdà, A., 1997. The effect of patchy distribution of *Stipa tenacissima* L. on runoff and erosion. Journal of Arid Environments, 36, 37–51.

Cerdà, A., 1998. The influence of aspect and vegetation on seasonal changes in erosion under rainfall simulation on a clay soil in Spain. Canadian Journal of Soil Science, 78, 321–330.

Cerdà, A., 2001. Effects of rock fragment on soil infiltration, inter-rill runoff and erosion. European Journal of Soil Science, 52, 1, 59–68.

Cerdà, A., 2002. The effect of season and parent material on water erosion on highly eroded soils in eastern Spain. Journal of Arid Environments, 52, 319–337.

Chen, G.X., Yao, W.Y., 1996. Effect of rainfall on hydraulic resistance of shallow flow. Advances in Water Science, 7, 42–46. (In Chinese with English Abstract.)

Chen, H.S., Shao, M.A., Li, Y.Y., 2008. Soil desiccation in the Loess Plateau of China. Geoderma, 143, 91–100.

De Baets, S., Poesen, J., Gyssels, G., Knapen, A., 2006. Effects of grass roots on the erodibility of topsoil during concentrated flow. Geomophology, 76, 54–67.

Dekker, S.C., Rietkerk, M., Bierkens, M.F.P., 2007. Coupling microscale vegetation-soil water and macroscale vegetation-precipitation feedbacks in semiarid ecosystems. Global Change Biology, 13, 671–678.

Dunkerley, D.L., Brown, K.J., 1995. Runoff and runon area in a patterned chenopod shrubland, arid western New South Wales, Australia: characteristics and origin. Journal of Arid Environment, 30, 41–55.

Dunkerley, D.L., Brown, K.J., 1999. Banded vegetation near Broken Hill, Australia: significance of surface roughness and soil physical properties. Catena, 37, 75–88.

Emmett, W.W., 1978. Overland flow. In: Kirkby, M.J. (Ed.): Hillslope Hydrology. John Wiley & Sons, New York, pp. 145–176.

Erpul, G., Norton, L.D., Gabriels, D., 2002. The effect of wind on raindrop impact and rainsplash detachment. ASAE, 46, 51–62.

Fan, C.C., Chen, Y.W., 2010. The effects of root architecture on the shearing resistance of root-permeated soils. Ecological Engineering, 36, 813–826.

Fowler, N., 1986. The role of competition in plant communities in arid and semiarid regions. Annual Review of Ecology and Systematics, 17, 89–110.

Giménez Morera, A., Ruiz Sinoga, J.D., Cerdà, A., 2010. The impact of cotton geotextiles on soil and water losses in Mediterranean rainfed agricultural land. Land Degradation & Development, 21, 2, 210–217.

Greenwood, J.E.G.W., 1957. The development of vegetation patterns in Somaliland Protectorate. Geographical Journal, 123, 465–473.

Guo, Z.S., 2000. Three coverages in vegetation construction for soil and water conservation: potential coverage, critical coverage, and effective coverage. Soil and Water Conservation in China, 4, 30–31. (In Chinese with English Abstract.)

Herbich, J.B., Shulits, S., 1964. Large-scale roughness in open-channel flow. Journal of the Hydraulics Division, 90,203–230.

Irvem, A., Topaloglu, F., Uygur, V., 2007. Estimating spatial distribution of soil loss over Seyhan River Basin in Turkey. J. Hydrol., 336, 30–37.

Jiang, C.B., Long, Y.N., Hu, S.X., Peng, Y.P., 2012. Recent progress in studies of overland flow resistance. Journal of Hydraulic Engineering, 43, 189–197. (In Chinese with English Abstract.)

Knapen, A., Smets, T., Poesen, J., 2009. Flow-retarding effects of vegetation and geotextiles on soil detachment during concentrated flow. Hydrological Processes, 23, 2427–2437.

Kröpfl, A.I., Cecchi, G.A., Villasuso, N.M., Distel, R.A., 2013. Degradation and recovery processes in Semi-Arid patchy rangelands of northern Patagonia, Argentina. Land Degradation & Development, 24, 393–399.

Lane, S.N., 2005. Roughness-time for a re-evaluation? Earth Surface Processes and Landforms, 30, 251–253.

Lawrence, D.S.L., 1997. Macroscale surface roughness and frictional resistance in overland flow. Earth Surface Processes and Landforms, 22, 365–382.

Lawrence, D.S.L., 2000. Hydraulic resistance in overland flow during partial and marginal surface inundation: experimental observations and modeling. Water Resource Research, 36, 8, 2381–2393.

Li, F.M., Xu, J.Z., Sun, G.Z., 2003. Restoration of degraded ecosystems and development of water-harvesting ecological agriculture in the semi-arid Loess Plateau of China. Acta Ecologica Sinica, 23, 1901–1915. (In Chinese with English Abstract.)

Li, G., 2009. Preliminary study of the interference of surface objects and rainfall in overland flow resistance. Catena, 78, 154–158.

Li, M., Yao, W.Y., Chen, J.N., Ding, W.F., 2007. Experimental study on runoff resistance of hilly slope-gullied surface with grass coverage. Journal of Hydraulic Engineering, 38,112–119. (In Chinese with English Abstract.)

Lieskovský, J., Kenderessy, P., 2014. Modelling the effect of vegetation cover and different tillage practices on soil erosion in vineyards: a case study in Vráble (Slovakia) using WATEM/SEDEM. Land Degradation & Development, 25, 288–296.

Luk, S.H., Merz, W., 1992. Use of the salt tracing technique to determine the velocity of overland flow. Soil Technology, 5, 289–301.

Luo, R.T., Zhang, G.H., Cao, Y., 2009. Progress in the research of hydrodynamic characteristics of sediment-laden overland flow. Progress in Geography, 28, 567–574. (In Chinese, with English Abstract)

Mei, X.P., 2004. Experimental study on hydrodynamic characteristics of sheet flow on slope under rain. Xi'an, Shaanxi: Xi'an University of Technology. (In Chinese with English Abstract.)

Nobel, S.P., 1990. Physicochemical and Environmental Plant Physiology. Second edition. Academic Press, London.

Pan, C.Z., Shangguan, Z.P., 2006. Runoff hydraulic characteristics and sediment generation in sloped grassplots under simulated rainfall conditions. J. Hydrol., 331, 178–185.

Pan, C.Z., Shangguan, Z.P., 2009. Experimental study on influence of rainfall and slope gradient on overland shallow flow hydraulics. Journal of Basic Science and Engineering, 17, 843–851.

Parsons, A.J., Abrahams, A.D., Wainwright, J., 1994. On determining resistance to interrill overland flow. Water Resources Research, 30, 3515–3521.

Puigdefábregas, J., 2005. The role of vegetation patterns in structuring runoff and sediment fluxes in drylands. Earth Surf. Process. Landforms, 30, 133–147.

Regües, D., Torri, D., 2002. Rainfall kinematics energy effect on physical properties dynamics and crusting of a clay bare soil. Cuaternarioy Geomorfología, 16, 57–71.

Roels, J.M., 1984. Flow resistance in concentrated overland flow on rough slope surface. Earth Surf. Process. Landforms, 9, 541–551.

Savat, J., 1977. The hydraulics of sheet flow on a smooth surface and the effect of simulated rainfall. Earth Surf. Process. Landforms, 2, 125–140.

Shen, H.W., Li, R.M., 1973. Rainfall effects on sheet flow over smooth surfaces. Journal of the Hydraulics Division, American Society of Civil Engineering, 99, 771–792.

Shoshany, M., 2012. Identifying desert thresholds by mapping inverse 2012 and recovery potentials in patch patterns using spectral and morphological algorithms. Land Degradation & Development, 23, 4, 331–338.

Smith, M.W., Cox, N.J., Bracken, L.J., 2007. Applying flow resistance equations to overland flows. Progress in Geography, 31, 363–387.

Vásquez-Méndez, R., Ventura-Ramos, E., Oleschko, K., Hernández-Sandoval, L., Parrot, J-F., Nearing, M.A., 2010. Soil erosion and runoff in different vegetation patches from semiarid Central Mexico. Catena, 80, 162–169.

Vásquez-Méndez, R., Ventura-Ramos, E., Oleschko, K., Hernández-Sandoval, L., Domínguez-Cortázar, M.A., 2011. Soil Erosion Processes in Semiarid Areas: The Importance of Native Vegetation. In: Godone, D. (Ed.): Soil Erosion Studies. In Tech, Rijeka, Croatia.

Wainwright, J., Parsons, A.J., Schlesinger, W.H., Abrahams, A.D., 2002. Hydrology–vegetation interactions in areas of discontinuous flow on a semi-arid bajada, Southern New Mexico. Journal of Arid Environments, 51, 319–338.

Wang, Y.Q., Shao, M.A., 2013. Spatial variability of soil physical properties in a region of the loess plateau of PR China subject to wind and water erosion. Land Degradation & Development, 24, 296–304.

Worrall, G.A., 1959. The Butana grass patterns. Journal of Soil Science, 10, 34–53.

Yi, Z.J., Yan, X.F., Huang, E., Liu, X.N., Wang, X.K., 2011. Calculation of overland flow resistance and hydraulic characteristics along slope distance in a steep experimental flume. Journal of Sichuan University (Engineering Science Edition), 43, 43–47.

Yoon, Y.N., Wenzel, H.G., 1971. Mechanics of sheet flow under simulated rainfall. Journal of the Hydraulics Division, American Society of Civil Engineering, 97, 1367–1386.

Zhang, G.H., 2012. Influence of patterned *Artemisia capillaris* on slope erosion and overland flow hydrodynamic characteristics [D]. Yangling, Shaanxi: Northwest A & F University. (In Chinese with English Abstract.)

Zhang, G.H., Luo, R.T., Cao, Y., Shen, R.C., Zhang, X.C., 2010. Impacts of sediment load on Manning coefficient in supercritical shallow flow on steep slopes. Hydrological Processes, 24, 3909–3914.

Zhang, G.H., Liu, G.B., Wang, G.L., 2012a. Effects of canopy and roots of patchy distributed *Artemisia capillaris* on runoff, sediment, and the spatial variability of soil erosion at the plot scale. Soil Science, 177, 409–415.

Zhang, G.H., Liu, G.B., Wang, G.L., Wang, Y.X., 2012b. Effects of patterned *Artemisia capillaris* on overland flow velocity under simulated rainfall. Hydrol. Process., 26, 3779–3787.

Zhang, K.L., 1999. Hydrodynamic characteristics of rill flow on loess slopes. Journal of Sediment Research, 1, 56–61. (In Chinese with English Abstract.)

Zhao, C.H., Gao, J.E., Xu, Z., 2013a. Mechanisms of grass in slope erosion control in loess sandy soil region of Northwest China. Chinese Journal of Applied Ecology, 24, 113–121. (In Chinese with English Abstract.)

Zhao, G., Mu, X., Wen, Z., Wang, F., Gao, P., 2013b. Soil erosion, conservation, and eco-environment changes in the Loess Plateau of China. Land Degradation & Development, 24, 499–510.

Zhou, Z.C., Shangguan, Z.P., 2007. The effects of ryegrass roots and shoots on loess erosion under simulated rainfall. Catena, 70, 350–355.

Ziadat, F.M., Taimeh, A.Y., 2013. Effect of rainfall intensity, slope and land use and antecedent soil moisture on soil erosion in an arid environment. Land Degradation & Development, 24, 582–590.

Received 21 April 2014
Accepted 11 August 2014